Preparation and Biomedical Applications of Bright Robust Silica Nanocapsules with Multiple Incorporated InP/ZnS Quantum Dots

Journal:	*New Journal of Chemistry*
Manuscript ID	NJ-ART-05-2018-002465.R2
Article Type:	Paper
Date Submitted by the Author:	10-Oct-2018
Complete List of Authors:	Li, Chunliang; Tianjin University of Technology; . National Institute of Advanced Industrial Science and Technology Hosokawa, Chie; National Institute of Advanced Industrial Science and Technology Suzuki, Mariko; National Institute of Advanced Industrial Science and Technology Taduchi, Takahisa; Center for information and neural networks (CiNet), National Institute of Information and Communications Technology (NICT) Murase, Norio; AIST, Health Research Institute

Preparation and Biomedical Applications of Bright Robust Silica Nanocapsules with Multiple Incorporated InP/ZnS Quantum Dots

Chunliang Li,[ab] Chie Hosokawa,[c] Mariko Suziki,[a] Takahisa Taguchi,[a†] Norio Murase[*a$]

[a]Health Research Institute, National Institute of Advanced Industrial Science and Technology (AIST), Ikeda, Osaka, 563-8577, Japan

[b]Tianjin Key Laboratory of optoelectronic materials and devices, School of Materials Science and Engineering, Tianjin University of Technology, Xiqing, Tianjin, 300384, People's Republic of China

[c]Biomedical Research Institute and Advanced Photonics and Biosensing Open Innovation Laboratory, National Institute of Advanced Industrial Science and Technology (AIST), Osaka, Japan

[†]Present affiliation: Center for information and neural networks (CiNet), National Institute of Information and Communications Technology (NICT), Suita, Osaka 565-0871, Japan

[$]Present affiliation: Kansai Collaboration Center, Kansai Center, National Institute of Advanced Industrial Science and Technology (AIST), Osaka, 563-8577, Japan. [*]E-mail:n-murase@aist.go.jp

Abstract

InP-based quantum dots (QDs) have been proposed as an alternative to CdSe-based QDs for both bioimaging and device displays. In this work, we incorporate hydrophilic InP/ZnS QDs into silica nanocapsules. The morphology, number of incorporated QDs, and photoluminescence (PL) properties of the capsules depend on the alkoxide hydrolysis conditions. By selecting a method of QD surface silanization, multiple QDs (typically 3) are incorporated into the nanocapsules (~40 nm in size) without causing significant deterioration of the initial PL efficiency (up to 36%). Degradation analysis in different buffer solutions indicates that silica nanocapsules have higher stabilities than pristine QDs. The surface of the nanocapsules was modified with carboxyl groups without any change in morphology. Bright PL images with high resolution were obtained after introducing the nanocapsules into rat hippocampal neurons, when compared with commercial Q-trackers (Polymer coated CdSe/ZnS).

1. Introduction

In recent years, nanomaterials have attracted widespread interest owing to their unique optical properties, which originate from the quantum confinement effect.[1,2] Colloidal quantum dots (QDs) have been studied widely as novel phosphors because of their properties such as broad absorption profiles, narrow tunable photoluminescence (PL) spectra, high photostability, and PL efficiency. These advanced properties led to their application in light-emitting and photovoltaic devices.[3–6] In biomedical applications, QDs often have significantly better photostability when compared with organic dyes.[7–9] With the rapid development of their synthesis, surface modification, and conjugation chemistry, together with better understanding of the interaction between QDs and biomolecules, QDs have been increasingly applied in biomedical fields such as cell imaging, diagnostics, and drug delivery.[10–16]

Currently, the brightest photoluminescent QDs are cadmium selenide (CdSe)-based QDs prepared in organic solvent, typically composed of a CdSe core and a zinc sulfide (ZnS) shell capped with hydrophobic ligands.[17–19] However, these QDs are not suitable for biomedical applications, primarily owing to their toxicity and poor water dispersity.[20,21] Preparation of hydrophilic QDs from initially hydrophobic QDs to improve biocompatibility has been a significant focus of recent research. Existing hydrophilic modification strategies include ligand exchange, amphiphilic polymer coating, and silica encapsulation. Ligand exchange of the hydrophobic molecules generally causes deterioration of the PL properties due to disruption of the atom locations at the surface,[7] and simple coating of QDs with polymers greatly increases their particle size.[22–25] Silica encapsulation is therefore an attractive approach to improving the water solubility and functionality required for bioconjugation. Silica encapsulation can also improve the photostability of QDs, reduce their cytotoxic effects, and improve biocompatibility.[26–28]

Indium phosphide (InP) is one of the most widely studied photoluminescent III–V QDs with a Bohr exciton radius of ~10 nm.[29] InP QDs are less toxic with robust

covalent bonds and tunable PL wavelength in the visible region (bulk bandgap *Eg*: 1.35 eV), which is similar to that of CdSe. The recent application of InP-based QDs in device displays was reported to be successful.[30–32] The most widely used method for InP QD synthesis is the dehalosilylation reaction between indium chloride ($InCl_3$) and tris(trimethylsilyl)phosphine ($P(Si(CH_3)_3)_3$) in the presence of a coordinating solvent.[33–36] After coating the InP core with a ZnS shell, the PL efficiency of InP/ZnS core-shell QDs in organic solvents increases by up to 40%.[36] Efforts have been made to improve the PL properties by optimizing the precursor materials as well as the synthesis procedures. The resultant InP QDs show PL efficiencies over 60%.[37–41] However, reports of the preparation of InP QDs in aqueous media were relatively rare until we reported a method for synthesizing highly luminescent InP/ZnS core-shell QDs in aqueous solution using a reactive phase transfer and photo-irradiation method.[42] The InP/ZnS QDs thus prepared showed band-edge PL that could be tuned from green to red with PL efficiencies of up to 68%.

Hydrophilic InP QDs are particularly important as a potential alternative to cadmium and lead based colloidal QDs in biomedical imaging. When CdSe/ZnS and InP/ZnS QDs were incubated with two cell types, the release of Cd^{2+} ions from CdSe induced cell mortality while InP QDs did not.[43] Compared with the CdTe/ZnS QD case, the cytotoxicity induced by reactive oxygen species (ROIs) was significantly lower in the case of InP/ZnS QDs.[44] Moreover, no discernable acute toxicity was observed after 12 weeks of intravenous injection of InP/ZnS QDs in mice.[45] Prasad and co-workers used a ligand exchange process to make hydrophobic InP/ZnS QDs highly dispersible in aqueous solution.[43] The resultant InP/ZnS QDs showed a PL efficiency of 30% and exhibited stable PL for more than 1 week when dispersed in common buffer solutions. These QDs could serve as targeted optical probes for several biomedical applications, including early detection of cancer.[46]

However, the molar extinction coefficient of InP QDs is approximately half that of CdSe QDs with the same radius.[47,48] Additional differences in PL spectral width, PL efficiency, and average PL lifetime lead to PL being an order of magnitude lower for InP/ZnS QDs compared with CdSe-based QDs when the excitation power is the

same. It is therefore difficult to detect the PL from single InP/ZnS QDs. Bright silica nanocapsules containing multiple QDs can detect in vivo molecular events with high spatial and time resolution without blinking owing to the averaging effect.[49] The silica layer also contributes to enhancing the photostability that is particularly required for in vivo two photon detection.[50]

We encapsulated both hydrophilic and hydrophobic QDs in a silica (or glass) matrix using various sol-gel processes.[51–53] Reaction in solution at room temperature is advantageous for the surface control of delicate QDs. Throughout the study the sol-gel matrix itself was found to control the resultant morphology through self-organization. Emitting silica matrices such as plates, fibers, thin films, and powders have thus been prepared.[54] We have also reported encapsulating CdSe/ZnCdS QDs (λ_{em}=620 nm) with hydrophobic ligands in silica capsules.[55,56] However, to date there have been no reports of incorporating multiple InP QDs into a single silica capsule.

In this study, silica nanocapsules containing multiple incorporated hydrophilic InP/ZnS QDs were prepared. Highly luminescent InP/ZnS QDs were first prepared through reactive phase transfer and photochemical processing,[42] then were incorporated into silica nanocapsules using a modified Stöber method. The surface differences between the silanized QDs result in variations in final morphology and PL properties. The preparation process was optimized in order to obtain silica nanocapsules with high PL efficiency, and nearly spherical morphology. Deterioration tests of the prepared nanocapsules were carried out in several buffer solutions in comparison with pristine InP/ZnS QDs. Furthermore, the nanocapsules were introduced into rat hippocampal neurons by endocytosis. The florescence images obtained by laser scanning confocal microscopy highlighted the possibility of using the nanocapsules for biomedical applications.

2 Experimental section

2.1 Materials

All chemicals were of analytical grade or the highest purity available, and used

directly without any further purification. Indium (III) chloride ($InCl_3$, 99.999%), dodecylamine (DDA, 98%), acetonitrile (99.9%), zinc perchlorate hexahydrate ($Zn(ClO_4)_2 \cdot 6H_2O$, 98%), and tetraethyl orthosilicate (TEOS, 97%), were purchased from Sigma-Aldrich. Thioglycolic acid (TGA, 90%), and tris(dimethylamino)phosphine ($P(N(CH_3)_2)_3$, 98%) were obtained from Wako Chemicals. Ammonium hydroxide and other organic solvents such as toluene, hexane, and methanol were also purchased from Wako Chemicals. The solvents used were of dehydrated grade. Dulbecco's modified Eagle's medium (DMEM) buffer, tris-borate-EDTA (TBE, 10X) buffer, and phosphate buffer solutions (PBS, 10X) were obtained from Sigma-Aldrich. Carboxyethylsilanetriol sodium (CES) was purchased from Gelest. 2-[4-(2-Hydroxyethyl)-1-piperazinyl]ethanesulfonic acid (HEPES) powder was from DOJINDO. Ultrapure deionized water (18.2 MΩ/cm) was obtained from a Milli-Q synthesis system (Millipore).

2.2 Synthesis of InP/ZnS QDs

InP/ZnS QDs were synthesized in three steps through reactive phase transfer and photochemical processing using a previously reported method.[42] First, hydrophobic InP cores were prepared in organic solvent using a solvothermal method. Typically, $InCl_3$, $P(N(CH_3)_2)_3$, and DDA were mixed with toluene and sealed in a Teflon-lined autoclave in a glovebox under an atmosphere of argon. The autoclave was then taken out of the glovebox and heated to 180°C for 24 h. The cooled solution was then slightly precipitated, and the byproducts were discarded. The obtained InP cores were subjected to size-selective precipitation using methanol and redispersed in hexane.

Second, the hydrophobic InP cores were transferred into aqueous solution. InP cores (1×10^{-6} mol) were dispersed in 2 mL of a hexane and butanol mixture (hexane/butanol=2:1). This solution was then mixed with 2 mL of a solution containing Zn^{2+} ions and TGA (Solution ZT). Solution ZT was prepared by dissolving $Zn(ClO_4)_2 \cdot 6H_2O$ and TGA in water; the pH of the solution was adjusted to 11.0. After stirring the mixture at 50°C for 1 h, the InP cores were completely transferred to the aqueous layer and the organic layer became transparent. The InP cores in the aqueous

solution were then precipitated and redispersed in 2 mL of Solution ZT for continued creation of a ZnS shell through post-preparative irradiation.

Finally, a ZnS shell was deposited on the surface of the InP cores through post-preparative irradiation with UV light (λ=365 nm, 3 W/cm^2) from a 250 W UV lamp in every case. Following irradiation, the InP/ZnS QDs were precipitated from the reaction mixture by adding acetonitrile and were redispersed in water.

Three kinds of InP/ZnS QDs were used with PL wavelengths of 597, 621, and 642 nm. The core size of these QDs were derived to be 3.0, 3.2, and 3.7 nm, respectively from the wavelength of the first absorption peak. (see Fig.S1 in Ref 42 for detail). The thickness of ZnS shell coated on each InP core was roughly 1.5 nm. The PL efficiencies of these QDs ranged from 32% to 52% (Table 1, TEM images of QD1 are shown in Fig. 7 in Ref. 42).

Table 1. PL properties of InP/ZnS QDs and silica nanocapsules with incorporated QDs.

No.	Structure	Method	PL wavelength λ / nm	PL efficiency η (%)	FWHM* / nm
1	QD1		597	32	77
2	QD2		621	45	95
3	QD3		642	52	83
4	QD2-SiO_2	M1-15min	627	9	96
5	QD2-SiO_2	M1-30min	619	12	92
6	QD2-SiO_2	M1-90min	622	5	103
7	QD1-SiO_2	M2	605	14	72
8	QD2-SiO_2	M2	626	20	94
9	QD3-SiO_2	M2	643	36	82

*Full Width at Half Maximum.

Scheme 1. Two procedures used for preparing silica nanocapsules with incorporated hydrophilic InP/ZnS QDs through the Stöber method. a) hydrolysis of TEOS in advance before addition of the QDs (M1); b) Silanization of QDs with partially hydrolyzed TEOS before addition of aqueous ammonia (M2).

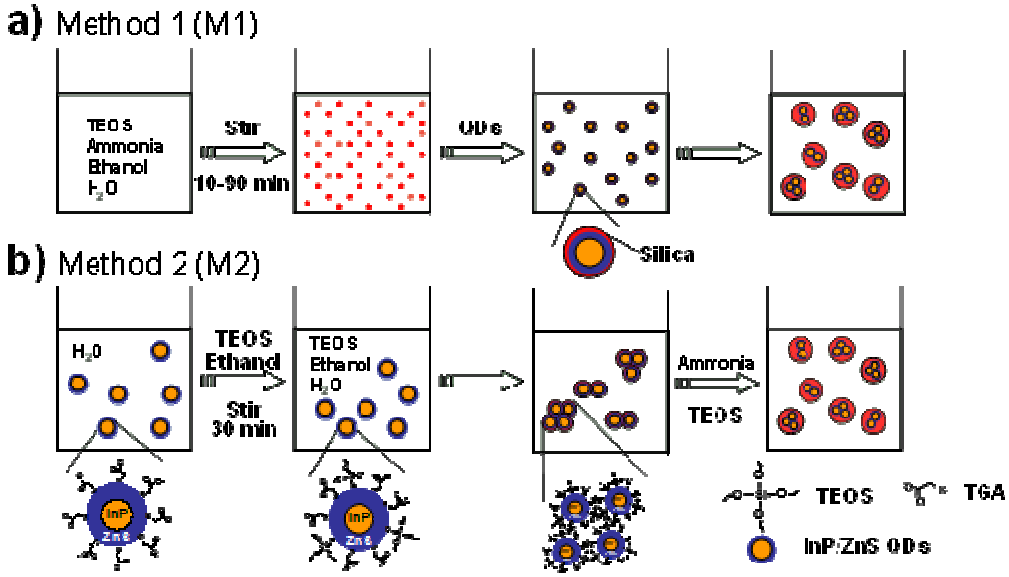

2.3 Preparation of silica nanocapsules with incorporated InP/ZnS QDs

The nanocapsules were prepared using two different Stöber methods (Scheme 1), which differed in the timing of the QD addition. All steps were carried out at room temperature. The concentration of InP/ZnS QDs was estimated using the previously reported absorption coefficient of InP QDs.[48]

The first method (M1) was a modified version of the aqueous Fe_3O_4 method.[58] Briefly, 4 mL of ethanol, 0.6 mL of water, 5 μL of TEOS, and 100 μL of aqueous ammonia (25wt%) were mixed, and stirred for several tens of minutes (15, 30 and 90 min) to partially hydrolyze the TEOS. Subsequently, 0.1 mL of InP/ZnS QD solution (3 μM) was added and the solution was stirred for a further 3 h. The silica nanocapsules were then precipitated and washed with ethanol several times. The final nanocapsules were redispersed in ultrapure water.

In the second method (M2), 0.1 mL of QD solution (3 μM) was diluted with 0.6 mL of water, then 4 mL of ethanol and 1 μL of TEOS were added to the solution at room temperature with stirring. The mixed solution was stirred for 1–3 h to ensure

that the surface of the InP/ZnS QDs was silanized with partially hydrolyzed TEOS molecules. Then 0.1 mL of aqueous ammonia (25wt%) was slowly added to the solution, and another 5 μL of TEOS was added for further SiO_2 shell coating. After stirring for 3 h, silica nanocapsules were precipitated, washed with ethanol, and redispersed in water.

2.4 Deterioration test of silica nanocapsules in buffer solutions

Silica nanocapsules with incorporated InP/ZnS QDs were added to three different buffer solutions; Dulbecco's modified Eagle's medium (DMEM), PBS (pH 7.4), and 2-[4-(2-hydroxyethyl)-1-piperazinyl]ethanesulfonic acid (HEPES) buffer. The concentration of QDs in the buffers was fixed at 10 nM. HEPES powder, NaOH solution (1 N), and pure water (Milli-Q) were used to make HEPES stock solution (10 mM, pH 7.4). The PL efficiencies of the QDs in the three buffers were then monitored over time.

2.5 Surface modification of silica nanocapsules with incorporated InP/ZnS QDs

Carboxyl surface modification of silica nanocapsules was carried out using carboxyethylsilanetriol sodium (CES) via a previously reported method.[59] Typically, an aliquot of silica nanocapsules was dispersed in 1 mL of 10 mM PBS (pH 7.4) with gentle stirring, followed by addition of 20 μL of CES (25% aqueous solution). After reacting at room temperature for 3–4 h, the modified nanocapsules were centrifuged and washed several times with PBS buffer.

2.6 Hippocampal neuron culture

The procedure was approved by the Institutional Animal Care and Use Committee at the National Institute of Advanced Industrial Science and Technology (AIST, Japan). Hippocampal neurons were isolated from 18-day-old embryos of a Wistar rat, dissociated by treatment with 0.1% trypsin, and plated at a density of 3.1×10^2 cell/mm^2 in a glass-bottomed dish. The dissociated neurons were maintained at a temperature of 37ºC in a humidified atmosphere containing 5% CO_2 and cultured in neurobasal medium containing a B-27 supplement (Thermo Fisher Scientific (Invitrogen)) and penicillin (60 μg/mL), streptomycin (100 μg/mL), and insulin (5

μg/mL).

2.7 Cell imaging using silica nanocapsules

The prepared silica nanocapsules were diluted with neurobasal medium and added gently to the glass-bottomed dishes containing rat hippocampal neurons. After an optimized incubation time of 1–3 h, silica nanocapsules in the solution were observed using a fluorescence microscope (Olympus IX71) equipped with an EM-CCD camera (Roper Scientific, PhotonMAX1024B). The observation of hippocampal neurons with silica nanocapsules using confocal laser scanning microscopy (CLSM) was carried out using an Olympus FV-300 equipped with an upright microscope (Olympus, BX-50WI). The excitation wavelength was set to 488 nm. Commercial cell labeling kits using polymer-coated CdSe/ZnS QDs (Q-tracker 655) were purchased from Thermo Fisher Scientific (Invitrogen), and used directly for observation using the same conditions.

2.8 Other Apparatus

Transmission electron microscopy (TEM) was performed using a Hitachi H-9000NA electron microscope operated at an accelerating voltage of 300 kV. The specimens were prepared by putting one drop of the nanocapsule solution onto the surface of high-resolution carbon-supported copper grids (pitch of 100 μm). UV-visible absorption spectra of the QDs were obtained using a spectrophotometer (U-4000, Hitachi). PL spectra measurements were acquired using a spectrofluorometer (F-4500, Hitachi) with an excitation wavelength of 400 nm.

The PL efficiencies of the QD and silica nanocapsule solutions were estimated based on a reported method using a standard solution of quinine in an aqueous 0.05 M H_2SO_4 solution (η =54.6%).[57] The PL efficiency was obtained from the absorbance and PL spectra measured using the conventional UV-VIS and fluorescence spectrophotometers described above.

3. Results and Discussion

3.1 Preparation of silica nanocapsules with incorporated InP/ZnS QDs

In a typical sol-gel process aqueous ammonia is commonly used to adjust the pH of the solution and accelerate the hydrolysis of TEOS. Solutions in the alkaline pH range are known to create spherical silica particles.[60] However, excess ammonia can affect the surface of the QDs and reduce the PL efficiency after silica coating.[61]

It was noted that the surface of both hydrophobic and hydrophilic QDs can be modified by substituting a proportion of the original ligands with partially hydrolyzed TEOS.[55,56,62] Surface modification makes interaction between the QDs and hydrolyzed TEOS molecules favorable, and allows facile formation of a silica layer on the surface. The silica layer can prevent the QDs from coming into close contact with conditions that would be detrimental to the surface, whilst retaining the original PL properties. Herein, hydrophilic InP/ZnS QDs were added to a solution in which TEOS was partially hydrolyzed, for further silica coating. Two methods (M1 and M2) were adopted by altering the timing of QD addition into the solution as explained below.

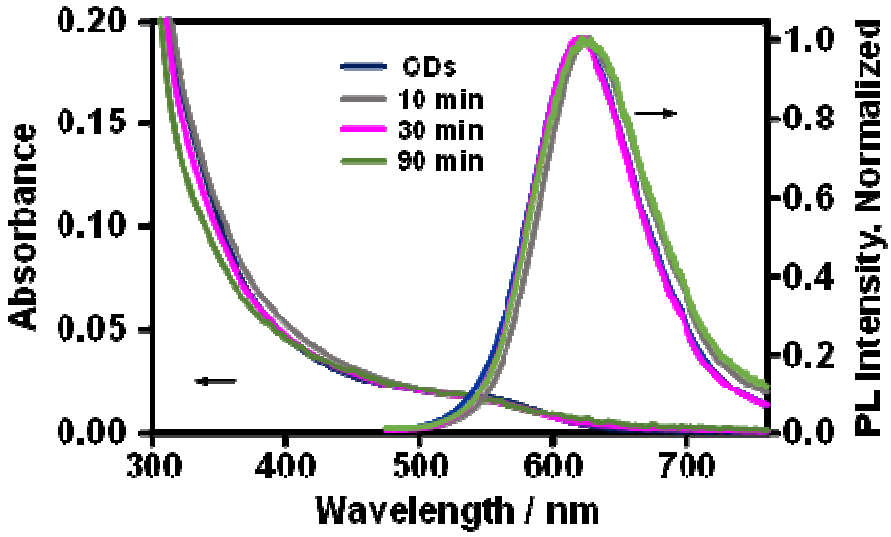

Figure 1. Absorption and PL spectra of InP/ZnS QDs in aqueous solution and in silica nanocapsules prepared following different TEOS advanced hydrolysis time periods (M1 method).

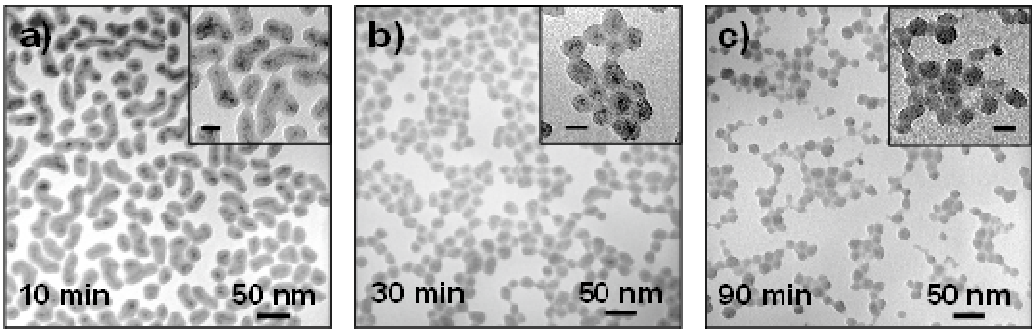

Figure 2. TEM images of silica nanocapsules obtained following different TEOS hydrolysis time periods (M1 method) (a) 10 min, (b) 30 min, and (c) 90 min. Insets show high-resolution images of silica capsules revealing the distribution of QDs. The scale bar in the inset corresponds to 20 nm.

In the M1 method (Scheme 1a), hydrophilic InP/ZnS QDs, which emit at one wavelength (621 nm), were added to a solution in which TEOS had been hydrolyzed in advance for different periods of time as shown in Table 1 (Samples 4–6). Figure 1 shows the absorption and PL spectra of the initial InP/ZnS QDs in water and after silica encapsulation. TEOS was hydrolyzed for 10, 30, or 90 min before combination with the QDs. Both the absorption and PL spectra remained unchanged after incorporation, except for a slight red shift of the PL peak wavelength. Figure 2 shows TEM images of the prepared nanocapsules. As the hydrolysis time was extended, the particle size was found to significantly decrease. The shapes of the particles also changed from irregular to spherical. When QDs were added after 10 min of TEOS hydrolysis, the particles were more than 50 nm in size with irregular shapes (Figure 2a). The enlarged image shows that several QDs were encapsulated with linear alignment into the particles. However, when the hydrolysis time was increased to 30 min, the particle size decreased to ~20 nm (Figure 2b). These nanocapsules have almost spherical shape and contain only 1 or 2 QDs per capsule. When TEOS was hydrolyzed for 90 min, the resulting nanocapsules were smaller (Figure 2c). It is difficult to clearly determine from the figure whether or not every particle contains QDs. In addition, gel-like materials were observed between the particles.

The significant differences in morphology observed were a result of the concentration of hydrolyzed TEOS molecules in the solution during the reaction. In the silica coating process a portion of ligand molecules (TGA) on the surface of the InP/ZnS QDs exchanged with hydrolyzed silica monomer, where the silica molecules were able to condense with other hydrolyzed silica monomers in the solution to form a silica network. When relatively fewer hydrolyzed silica monomers were in the solution, no small silica particulates appeared. In this case, the above-mentioned ligand exchange proceeds accompanied by alignment of QDs because of the polar nature of ethanol. It has been shown that thiol-capped QDs self-assemble linearly in aqueous solution to form one dimensional nanowires.[63] The hydrolyzed silica molecules deposited partially on the surface of the QDs led to the formation of the observed silica nanoparticles containing more than two InP/ZnS QDs.

When TEOS was hydrolyzed for ~30 min, sufficient hydrolyzed silica monomers were available in solution, therefore each QD was rapidly coated with a silica layer leading to singlet or doublet QDs in the capsules. The obtained silica nanocapsules were essentially spherical in shape and contained 1 or 2 QDs per capsule. When the hydrolysis time was increased to 90 min, an excess of hydrolyzed silica molecules was present, which condensed into small silica particulates independently before addition of the InP/ZnS QDs. The silica particulates were small silica particles containing no InP/ZnS QDs. These findings are similar to those reported for aqueous Fe_3O_4, for which small particles were obtained when the hydrolysis time exceeded 40 min.[58]

The PL properties of QDs before and after their incorporation into nanocapsules are shown in Table 1 (Samples 4–6). The nanocapsules show PL efficiencies of 9%, 12%, and 5% with hydrolysis times of 10, 30, and 90 min, respectively. These values are significantly lower than those of the initial QDs. In addition, the peak wavelengths and the full width at half maximum (FWHM) also varied for different hydrolysis times. The PL efficiencies are directly related to the conditions of the QDs after incorporation into the nanocapsules. When the QDs were added after 30 min of hydrolysis, the obtained nanocapsules, in which one or two QDs were incorporated

per nanocapsule, showed the highest PL efficiency. When QDs were added after 90 min of hydrolysis, the PL efficiency became much lower, probably as a result of the deterioration of the surface. The general tendency is for PL efficiency to decrease when the TEOS monomer exchanges with the original ligand more slowly.[55] The PL wavelength shifts to the red due to excitation energy transfer and reabsorption of PL between QDs assembled closely (linearly in the present case). This causes the PL efficiency to deteriorate by forming imperfect bonding with adjacent QDs.

In order to prevent a decrease in PL efficiency, the surfaces of QDs emitting three PL wavelengths were initially silanized by TEOS using the M2 method (Scheme 1b, Samples 7–9 in Table 1). In this method, InP/ZnS QDs were mixed with partially hydrolyzed TEOS for several hours to exchange the surface ligands at a moderate speed, which led to assemblies of QDs without agglomeration. Subsequent addition of aqueous ammonia accelerates the hydrolysis of TEOS to create the nanocapsules.

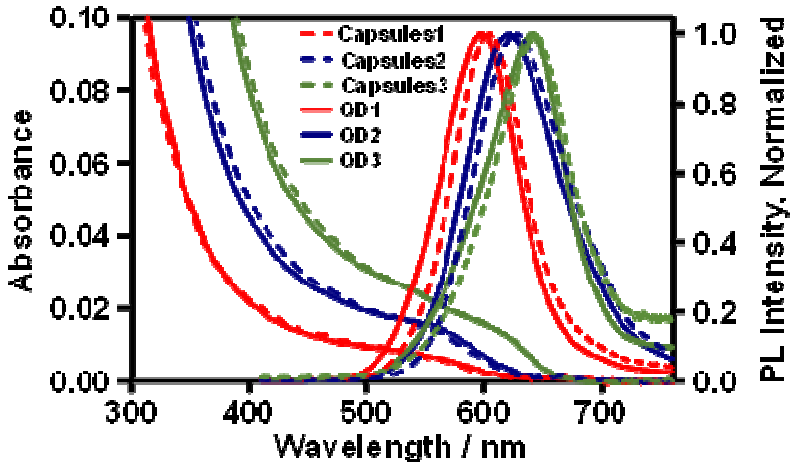

Figure 3. Absorption and PL spectra of InP/ZnS QDs in solution and in silica nanocapsules prepared using a Stöber method with silanized QDs (M2 method). The PL peak wavelengths of the QDs after incorporation were 605, 626, and 643 nm, respectively.

Figure 3 shows normalized absorption and PL spectra of InP/ZnS QDs in aqueous solution and in the nanocapsules prepared using the M2 method. Both the

absorption and PL spectra remained unchanged after incorporation except for a slight red-shift of the PL peak wavelength. The PL wavelength of smaller QDs goes to the red more because of their greater reduction of quantum confinement effect. Table 1 shows that the nanocapsules that emit in the orange region (605 nm) showed PL efficiency of approximately half that of the initial QDs. However, the PL efficiency of the nanocapsules that emit in the red region (643 nm) reached 36%, which is roughly 70% of the original efficiency. These nanocapsule PL efficiencies are similar to those of silica capsules with incorporated hydrophobic CdSe/ZnCdS QDs.[56] The PL efficiencies obtained for the M2 capsules were significantly higher than those of the nanocapsules prepared by the M1 method as shown in Table 1. This result shows that the surface modification of QDs with silicon alkoxides should ideally be slow in order to retain the PL efficiency. The surface modification of QDs in the M2 method forms a silica layer on the surface. This layer makes the silica monomers condense onto the QDs, which protects the PL from decreasing during capsule formation. The general tendency shown by Samples 7–9, is for larger size QDs to show less of a decrease in PL. This is because the effect of surface deterioration on PL efficiency is less marked when the core size of the QDs becomes larger. Further optimization of the silica coating process could maximize the PL efficiency.

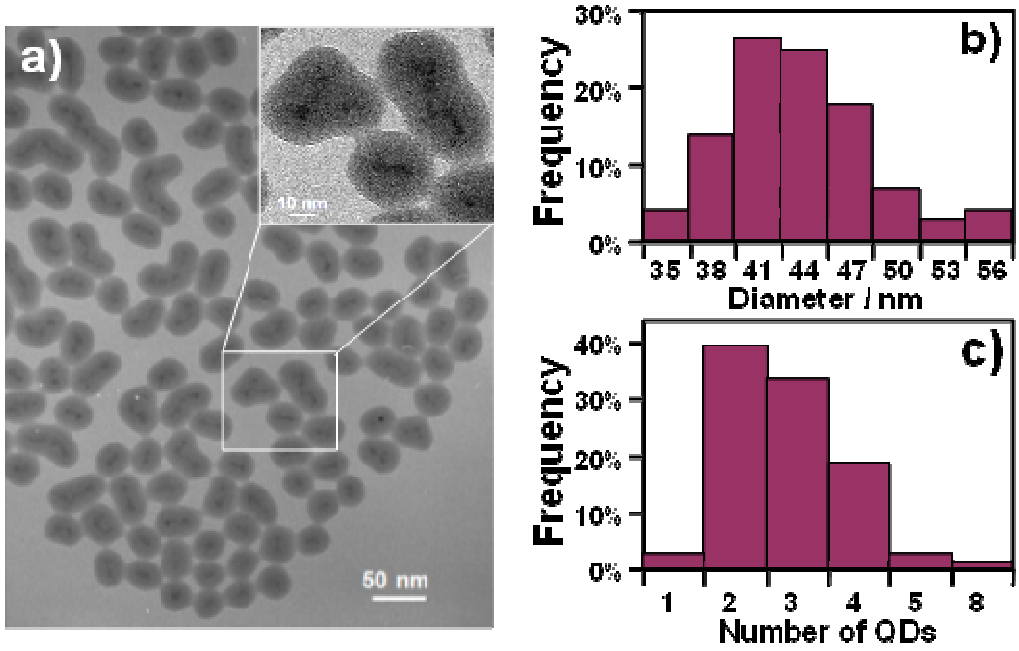

Figure 4. (a) TEM images of silica nanocapsules prepared by the Stöber method using silanized QDs (M2 method). The inset shows a high-resolution image revealing the distribution of the QDs. (b) Size-distribution of silica nanocapsules. (c) Distribution of the numbers of QDs in each silica nanocapsule. The PL peak wavelength of the QDs was 626 nm (Sample 8).

Figure 4a shows TEM images of the nanocapsules prepared using the M2 method (Sample 8). The nanocapsules are essentially spherical and the QDs are well dispersed within the capsules. The enlarged high-resolution image (Figure 4a, inset) clearly shows the distribution of the QDs in the nanocapsules. The size distributions of the nanocapsules are depicted in Figure 4b. The average particle size is 42±5 nm. Figure 4c shows that the number of QDs in each nanocapsule is 3.0±1.3. This is less than the previous report on silica capsules with incorporated hydrophobic CdSe/ZnCdS QDs, where more than 15 QDs were encapsulated per capsule.[55,56] However, the current result shows the morphology similar to the silica capsules incorporating other hydrophilic QDs[53] and Au nanoparticles[64], in which roughly the

same number of nanoparticles are incorporated. The number of QDs inside the silica capsules shows the degree of QD self-assembly, which was regulated by the fabrication time of the silica nanocapsules. Therefore, the number of QDs inside the silica nanocapsules was similar to the reported results because the Stöber process was ~3 h in each case. We previously prepared silica nanocapsules that incorporated multiple aqueous CdTe QDs.[62] In that case, the hydrodynamic diameter was compared with that obtained by TEM. Since silica is harder than polymer, the hydrodynamic diameter was found to be the same as the diameter derived from TEM. Because the same Stöber method was applied in this work, we can say that the hydrodynamic diameter is also the same as that derived from TEM in this case.

Since the nanocapsules prepared by M2 showed better optical properties than the M1 samples, the following characterization was carried out for M2 nanocapsules only, unless explicitly stated otherwise.

3.2 Stability of silica nanocapsules with incorporated InP/ZnS QDs in buffer solutions

The deterioration of the silica nanocapsules (Sample 8 in Table 1) was compared with pristine InP/ZnS QDs (Sample 2, same PL wavelength as Sample 8) in various buffer solutions. The concentration of QDs in the buffer solutions was fixed at 10 nM.

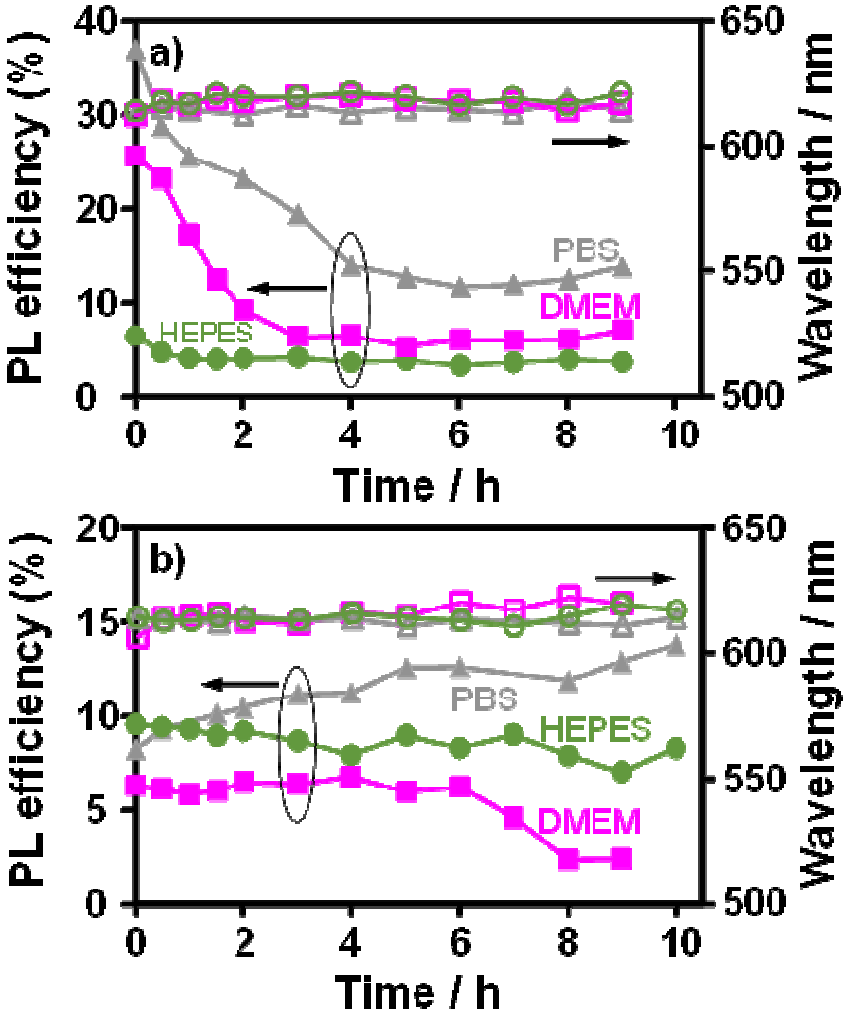

Figure 5. (a) Time-dependent PL efficiency and peak wavelength of InP/ZnS QDs in various buffer solutions. (b) Time course of PL efficiency and peak wavelength of silica nanocapsules in the same buffer solutions.

Figure 5a shows pristine InP/ZnS QDs. The peak wavelength of InP/ZnS QDs remained unchanged for several hours, whereas the efficiency dropped dramatically within 3 h. Among the three buffers, QDs in HEPES buffer were the worst affected; PL efficiency decreased to ~3%. QDs in PBS showed greater stability than those in DMEM buffer. Considering that the initial PL efficiency of InP/ZnS QDs is more than 40%, this result showed that the pristine InP/ZnS QDs are greatly affected by

physiological conditions. This reduction in PL efficiency was likely to be a result of changes in the TGA on the surface due to reaction with ions in the buffers, which could lead to the surfactant becoming inefficient as a passivating shell. Moreover, the extra ions in the buffer might cause the agglomeration of the QDs.

Figure 5b shows silica nanocapsules. The peak wavelength of the silica nanocapsules also showed minimal change over several hours. However, the stabilities were significantly improved compared with the pristine QDs. The PL efficiencies maintained their original values even after 6–7 h. PL efficiency in PBS showed a slight increase, possibly as a result of the recovery of the surface state of the QDs. This result shows that the silica coating greatly improved the stability and biocompatibility of the QDs.

3.3 Cell imaging using silica nanocapsules with incorporated InP/ZnS QDs

Silica nanocapsules in neurobasal medium were used to stain living rat hippocampal neurons through endocytosis. Observations were carried out using confocal laser scanning microscopy (CLSM). Figures 6a–6c show images of the nanocapsules in hippocampal neurons observed by CLSM at different Z-positions (from 0 to −6 μm). Figure 6d is the combined image (Z_{all}) of these results. From these images it can be seen that the neuron cells co-cultured with silica nanocapsules maintain their typical neuronal cell morphology. The fluorescence image also revealed that the nanocapsules showed strong fluorescence, and were distributed throughout the neuron cell. The bright and clear image revealed detailed information on the structure of the neuronal networks. The different Z-positions of the scan images established different information, and the combined picture consists of high resolution images that are almost the same as the transmission image (Figure 6e).

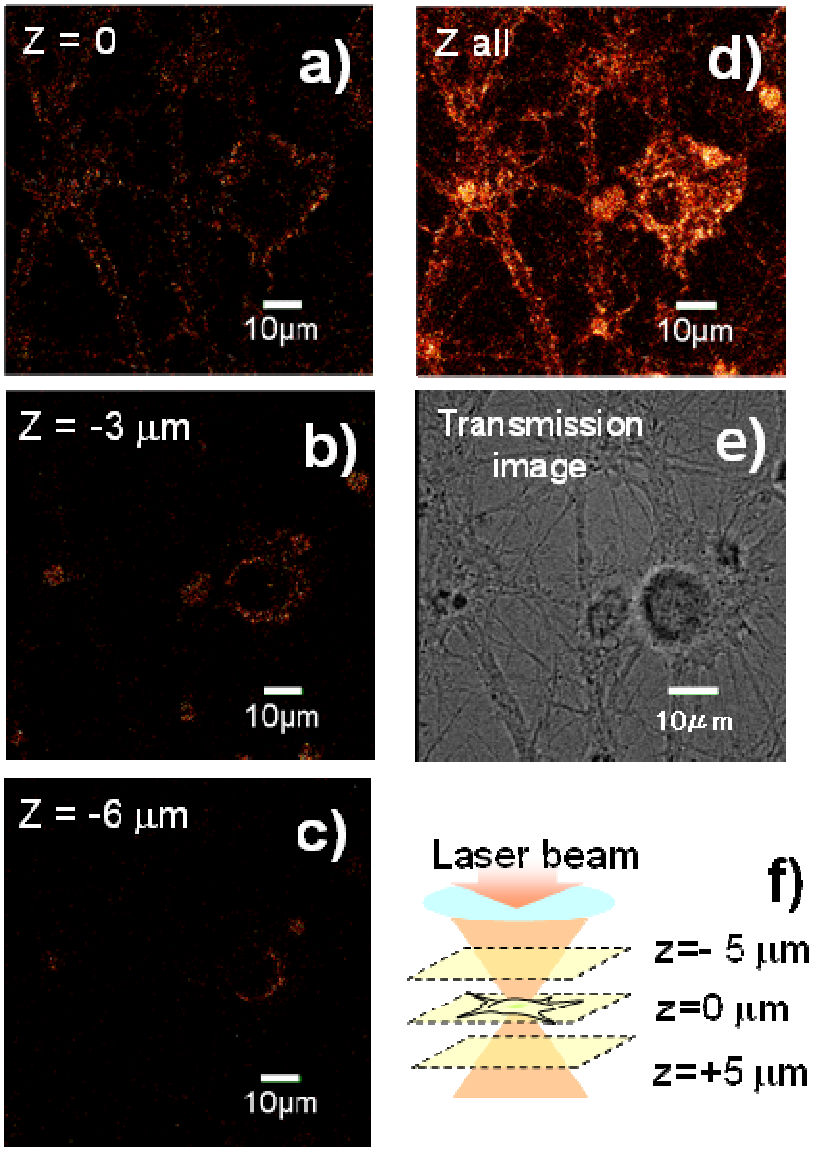

Figure 6. Confocal microscopy images of silica nanocapsules in rat hippocampal neurons. (a, b, c) Fluorescence images obtained at Z-positions of 0 μm, –3 μm, and –6 μm, respectively. (d) Composite of all fluorescence images obtained from various Z-positions. (e) Transmission image of nanocapsules in hippocampal neurons. (f) Scheme of Z-section scanning mode of CLSM.

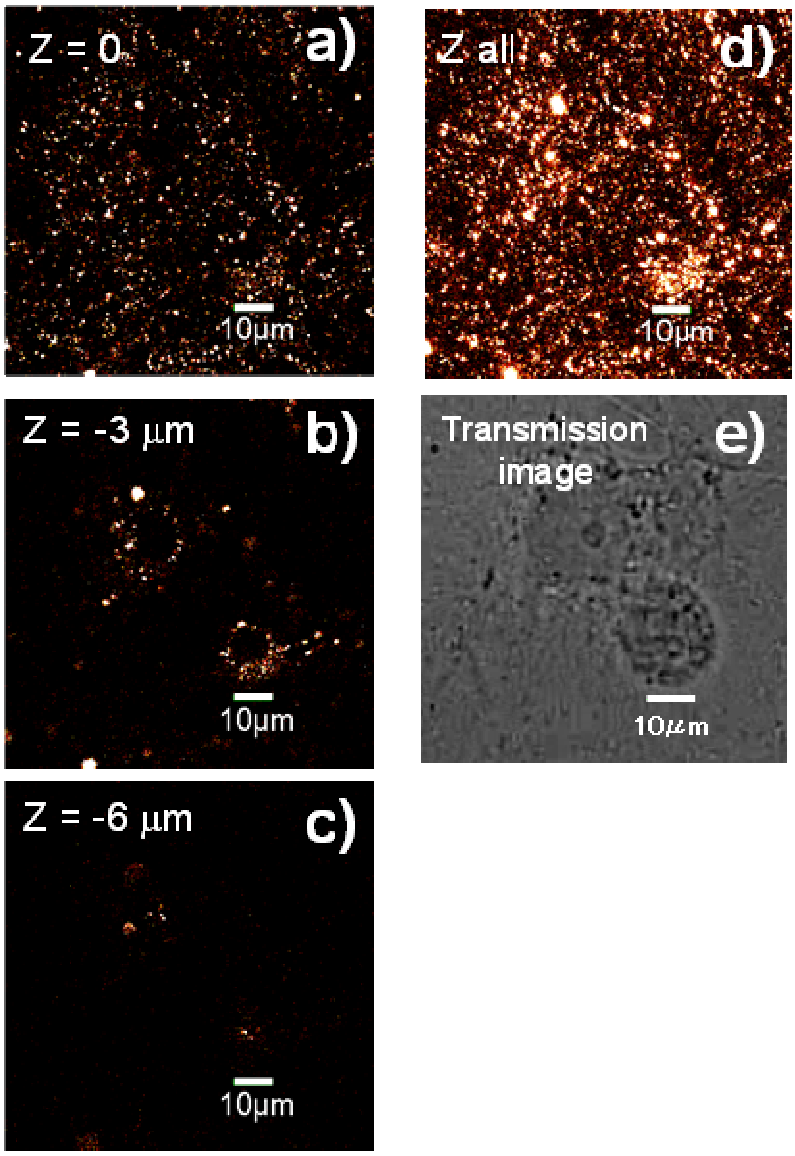

Figure 7. Confocal microscopy images of commercial cell labeling kit (Q-tracker 655) in rat hippocampal neurons. (a, b, c) Fluorescence images obtained at Z-positions of 0 μm, –3 μm, and –6 μm, respectively. (d) Composite image of all fluorescence images obtained from various Z-positions. (e) Transmission image of Q-tracker in hippocampal neurons.

However, there are clear differences when compared with the images of neurons stained using commercial labeling kit Q-trackers (Figures 7a–7c). Most of the

commercial QDs were trapped at the node of the neuronal network, not dispersed homogeneously. Though the PL intensity was relatively strong, the structure of the neuronal network was difficult to identify from the combined image (Z_{all}, Figure 7d) of the Z-section images. The transmission image (Figure 7e) clearly shows the difference when compared with the fluorescence images acquired by CLSM. Therefore, the silica nanocapsules prepared in this work show better performance for in vitro imaging than the commercial labels and provide detailed information on the morphology and structure of the neuron network. These results indicate that the nanocapsules show promise for biomedical imaging.

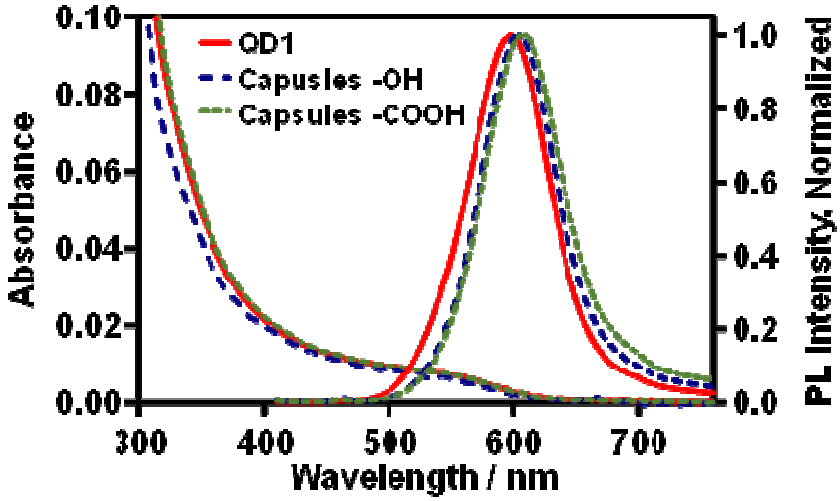

Figure 8. Absorption and PL spectra of InP/ZnS QDs in solution and in nanocapsules with surfaces modified with –OH and –COOH functional groups.

The surface of nanocapsules (OH) can be easily modified with other functional groups. Figure 8 shows the absorption and PL spectra of nanocapsules with hydroxyl (before modification) and carboxyl (after modification) functional groups on the surface, as well as the initial QDs. Both the absorption and PL spectra remained unchanged when the surface was modified from –OH to –COOH groups. The PL efficiency of the nanocapsules decreased slightly after the modification as shown in Table 2. TEM observation clarified that the shapes of the nanocapsules remained

almost unchanged. Neuronal cell imaging using the capsules before and after carboxyl group replacement, is shown in Figures 9a and 9b. The untreated nanocapsules (–OH surface) dispersed uniformly in the neuronal cells, while the nanocapsules with –COOH groups gathered together mainly at the primary node of the cell. This result indicates that the functional group replacement process was relatively successful. The ease of surface modification of the nanocapsules also supports their potential use in biomedical imaging.

Table 2. PL properties of InP/ZnS QDs and silica nanocapsules with different surface modifications prepared using the M2 method.

No.	Structure	Surface	PL wavelength λ / nm	PL efficiency η (%)	FWHM / nm
1	QD1	TGA	597	32	77
2	QD1-SiO_2	-OH	605	14	72
3	QD1-SiO_2	-COOH	606	12	76

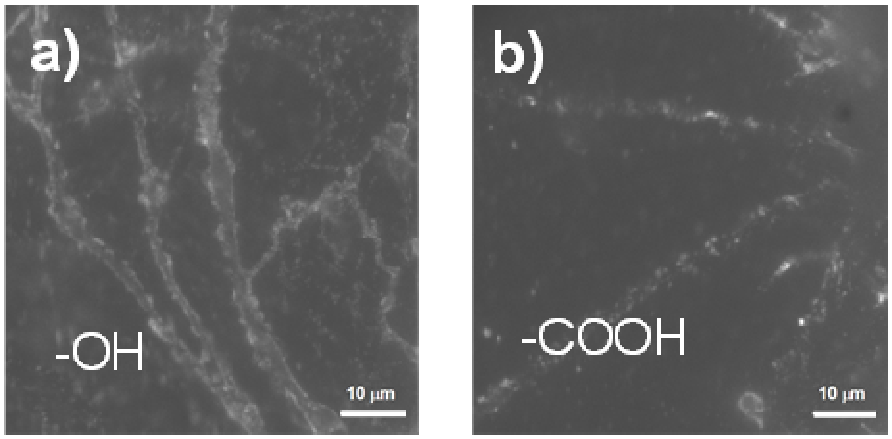

Figure 9. Epifluorescent image of rat hippocampal neurons stained with nanocapsules with different surface functional groups; (a) –OH and (b) –COOH.

Finally, we have to mention here that the quality (PL efficiency and spectral width) of the InP-related QDs are improved for example to add Ga together with In.[65] The silica-encapsulation method presented here stays valid for such InP-related QDs with higher quality of as well.

4. Conclusions

Silica nanocapsules containing multiple low-toxicity, water-soluble InP/ZnS QDs were prepared using two different methods. In the first method (M1), the QDs were added to a solution of TEOS that had been hydrolyzed in advance. Different nanocapsules morphologies were obtained for different hydrolysis times. The PL efficiencies of these capsules showed significant deterioration (5% or so). In the second method (M2), the surface of the QDs was silanized with TEOS before incorporation into capsules. The resulting nanocapsules had good morphology with multiple QDs (~3) incorporated per capsule, while their efficiency was maintained up to 36%. Degradation of the pristine QDs and these nanocapsules in buffer solutions indicated that the QDs embedded in the nanocapsules had good stability. The hydroxyl group surface of the nanocapsules could be easily modified to carboxyl groups, while the capsule morphology remained unchanged. The prepared nanocapsules were introduced into rat hippocampal neurons through endocytosis, and were observed by confocal laser scanning microscopy. The obtained bright and clear fluorescence images indicated that the nanocapsules are potential candidates for biomedical applications.

Conflicts of interest

There are no conflicts to declare.

Acknowledgments

This work was supported in part by CREST (Core Research for Evolutionary Science and Technology) from JST (Japan Science and Technology Agency), the Supporting Industry Program sponsored by METI (Ministry of Economy, Trade and Industry, Japan). We are grateful to Drs. Kazunori Kawasaki and Takeyuki Uchida for electron microscopy, and Dr. Masanori Ando for helping with the experiments. We are also grateful to Mrs. Qian Shi for her help on processing of the experimental data.

References

1 A.P. Alivisatos, *Science*, 1996, **271**, 933-937.
2 A.P. Alivisatos, *J. Phys. Chem*., 1996, **100**, 13226-13239.
3 S. Coe, W.K.Woo, M. Bawendi, and V. Bulovic, *Nature*, 2002, **420**, 800-803.
4 V.L. Colvin, M.C. Schlamp, and A.P. Alivisatos, *Nature*, 1994, **370**, 354-357.
5 M. Shalom, Z. Tachan, Y. Bouhadana, H.N. Barad, and A. Zaban, *J. Phys. Chem. Lett.*, 2011, **2**, 1998-2003.
6 H. Li, Q. Zhang, S. Zhou, and Q. Li, *RSC Adv.*, 2015, **5**, 30617-30623.
7 W.C.W. Chan, and S.M. Nie, *Science*, 1998, **281**, 2016-2018.
8 X.H. Gao, L. Yang, J.A. Petros, F.F. Marshall, J.W. Simons, and S.M. Nie, *Curr. Opin. Biotechnol*., 2005, **16**, 63-72.
9 X. Michalet, F.F. Pinaud, L.A. Bentolila, J.M. Tsay, S. Doose, J.J. Li, G. Sundaresan, A.M. Wu, S.S. Gambhir, and S. Weiss, *Science*, 2005, **307**, 538-544.
10 A. Verma, O. Uzun, Y. Hu, H.S. Han, N. Watson, S. Chen, D.J. Irvine, and F. Stellacci, *Nat. Mater*., 2008, **7**, 588-595.
11 Z.J. Zhu, R. Carboni, M.J. Quercio, B. Yan, O.R. Miranda, D.L. Anderton, K.F. Arcaro, V.M. Rotello, and R.W. Vachet, *Small*, 2010, **6**, 2261-2265.
12 M.L. Chen, Y.J. He, X.W. Chen, and J.H. Wang, *Langmuir*, 2012, **28**, 16469-16476.
13 H. Ding, F. Du, P. Liu, Z. Chen, and J. Shen, *ACS Appl. Mater. Interfaces*, 2015, **7**, 6889-6897.
14 N. Jia, Q. Lian, H. Shen, C. Wang, X. Li, and Z. Yang, *Nano Lett.*, 2007, **7**, 2976-2980.
15 T. Kim, M. Noh, H. Lee, S.W. Joo, and S.Y. Lee, *J. Phys. Chem. B*, 2009, **113**, 14487-14490.
16 C.P. Soman, and T.D. Giorgio, *Langmuir*, 2008, **24**, 4399-4404.
17 C.B. Murray, D.J. Norris, and M.G. Bawendi, *J. Am. Chem. Soc.*, 1993, **115**, 8706-8715.
18 D.V. Talapin, A.L. Rogach, A. Kornowski, M. Haase, and H. Weller, *Nano Lett.*, 2001, **1**, 207-211.
19 I. Mekis, D.V. Talapin, A. Kornowski, M. Haase, and H. Weller, *J. Phys. Chem. B*, 2003, **107**, 7454-7462.
20 A.M. Derfus, W.C.W. Chan, and S.N. Bhatia, *Nano Lett.* 2004, **4**, 11-18.
21 H.C. Fisher, and W.C.W. Chan, *Curr. Opin. Biotechnol.*, 2007, **18**, 565-571.
22 S.W. Kim, S. Kim, J.B. Tracy, A. Jasanoff, and M.G. Bawendi, *J. Am. Chem. Soc.*, 2005, **127**, 4556-4557.
23 B. Dubertret, P. Skourides, D.J. Norris, V. Noireaux, A.H. Brivanlou, and A. Libchaber, *Science*, 2002, **298**, 1759-1762.
24 X. Gao, Y. Cui, R.M. Levenson, L.W.K. Chung, S. Nie, *Nature Biotechnol.,* 2004, 22, 969-976.
25 W. Guo, J.J. Li, Y.A. Wang, and X.G. Peng, *Chem. Mater.*, 2003, **15**, 3125-3133.
26 D. Gerion, F. Pinaud, S.C. Williams, W.J. Parak, D. Zanchet, S. Weiss, and A.P. Alivisatos, *J. Phys. Chem. B*, 2001, **105**, 8861-8871.
27 A.L. Rogach, D. Nagesha, J.W. Ostrander, M. and N.A. Giersig, Kotov, *Chem. Mater.*, 2000, **12**, 2676-2685.
28 C. Kirchner, T. Liedl, S. Kudera, T. Pellegrino, A.M. Javier, H.E. Gaub, S. Stolzle, N. Fertig, and W.J. Parak, *Nano Lett.*, 2005, **5**, 331-338.
29 M. Green, *Curr. Opin. Solid State Mater. Sci.*, 2002, **6**, 355-363.
30 H. Wang, H. Zhang, H. Chen, H. Yeh, M. Tseng, R. Chung, S. Chen, and R. Liu, Small, 2017, 1603962.
31 H. Kim, Y. Park, J. Kim, C. Han, J. Lee, Y. Kim, T. Greco, C. Ippen, A. Wedel, B. Ju, and M.

Oh, *Adv. Funct. Mater.*, 2016, **26**, 3454–3461.
32 Quantum Dots: Solution for a Wider Color Gamut, https://pid.samsungdisplay.com/en/printpdf/386, accessed January, 2018.
33 O.I. Mićić, C.J. Curtis, K.M. Jones, J.R. Sprague, and A.J. Nozik, *J. Phys. Chem.*, 1994, **98**, 4966-4969.
34 A.A. Guzelian, J.E.B. Katari, A.V. Kadavanich, U. Banin, K. Hamad, E. Juban, A.P. Alivisatos, R.H. Wolters, C.C. Arnold, and J.R. Heath, *J. Phys. Chem*., 1996, **100**, 7212-7219.
35 O.I. Mićić, S.P. Ahrenkiel, and A.J. Nozik, *Appl. Phys. Lett.*, 2001, **78**, 4022-4024.
36 R. Xie, D. Battaglia, X.G. Peng, *J. Am. Chem*. Soc., 2007, **129**, 15432-15433.
37 M.D. Tessier, D. Dupont, K. De Nolf. J. De, Roo, and Z. Hens, *Chem. Mater.*, 2015, **27**, 4893-4898.
38 F. Zan, and J. Ren, *J. Mater. Chem.*, 2012, **22**, 1794-1799.
39 S. Xu, J. Ziegler, and T. Nann, *J. Mater. Chem.*, 2008, **18**, 2653-2656.
40 X. Yang, D. Zhao, K.S. Leck, S.T. Tan, Y.X. Tang, J. Zhao, H.V. Demir, and X.W. Sun, *Adv. Mater.*, 2012, **24**, 4180-4185.
41 L. Li, and L. Reiss, *J. Am. Chem. Soc.*, 2008, **130**, 11588-11589.
42 C.L. Li, M. Ando, H. Enomoto, and N. Murase, *J. Phys. Chem. C*, 2008, **112**, 20190-20199.
43 V. Brunetti, H. Chibli, R. Fiammengo, A. Galeone, M.A. Malvindi, G. Vecchio, R. Cingolani, J.L. Nadeau, and P.P. Pompa, *Nanoscale*, 2013, **5**, 307-317.
44 H. Chibli, L. Carlini, S. Park, N.M. Dimitrijevic, and J.L. Nadeau, *Nanoscale*, 2011, **3**, 2552-2559.
45 G. Lin, Q. Ouyang, R. Hu, Z. Ding, J. Tian, F. Yin, G. Xu, Q. Chen, X. Wang, and K.T. Yong, *Nanomedicine*, 2015, **11**, 341-350.
46 K. Yong, H. Ding, I. Roy, W. Law, E.J. Bergey, A. Maitra, and P.N. Prasad, *ACS Nano*, 2009, **3**, 502-510.
47 W.W. Yu, L. Qu, W. Guo, and X. Peng, *Chem. Mater.*, 2003**, 15**, 2854-2860.
48 S. Adam, D.V. Talapin, H. Borchert, A. Lobo, C. McGinley, A.R.B. de Castro, M. Haase, H. Weller, and T. Moller, *J. Chem. Phys.*, 2005**, 123**, 084706.
49 CREST Project Report, http://www.jst.go.jp/kisoken/crest/research/s-houkoku/02_03.pdf, accessed January, 2018, In Japanese
50 D.J. Bharali, D.W. Lucey, H. Jayakumar, H.E. Pudavar, and P.N. Prasad, *J. Am. Chem. Soc.*, 2005, **127**, 11364-11371.
51 C.L. Li and N. Murase, *Langmuir***,** 2004**, 20,** 1-4.
52 P. Yang, M. Ando, T. Taguchi, and N. Murase, *J. Phys. Chem. C*, 2011**, 115**, 14455-14460.
53 P. Yang, and N. Murase, *ChemPhysChem***,** 2010**, 11**, 815 -821.
54 N. Murase, in *Nanomaterials for the Life Sciences*, Edited by Challa S. S. R. Kumar, ILEY-VCH, Weinheim, 1st edition, 2010, Chapter 11, pp 393-428.
55 P. Yang, N. Murase, M. Suzuki, C. Hosokawa, K. Kawasaki, T. Kato, T. Taguchi, *Chem. Commun.***,** 2010**, 46**, 4595 -4597.
56 C.L. Li, and N. Murase, *J. Colloid Interf. Sci.***,** 2013**, 411**, 82-91.
57 N. Murase, and C.L. Li, *J. Lumin.*, 2008**, 128**, 1896-1903.
58 Z. Lu, J. Dai, X. Song, G. Wang, W. Yang, *Colloid. Surf. A*., 2008**, 317**, 450 -456.
59 G.T. Hermanson, *Bioconjugate Techniques Second Edition,* Academic Press, San Diego, 2008.
60 C.J.Brinker, and G.W. Scherer, *Sol-Gel Science,* Academic Press, San Diego, 1990.
61 R. Koole, M.M. Schooneveld, J. Hilhorst, C.D. Donega, D.C. Hart, A.V. Blaaderen D. Vanmaekelbergh, and A. Meijerink, *Chem. Mater.*, 2008**, 20**, 2503-2512.
62 P. Yang, M. Ando, and N. Murase, *J. Colloid. Interf. Sci*., 2007**, 316,**, 420-427.

63 Z. Tang, N.A. Kotov, and M. Giersig, *Science*, 2002**, 297**, 237-240.

64 P. Yang, M. Ando, and N. Murase, *Langmuir*, 2011**, 27**, 895-901.

65 S. Kim, T. Kim, M. Kang, S. K. Kwak, T. W. Yoo, L. S. Park, I. Yang, S. Hwang, J. E. Lee, S. K. Kim, S.-W. Kim, *J. Am. Chem. Soc.* 2012, **134,** 3804−3809.

TOC

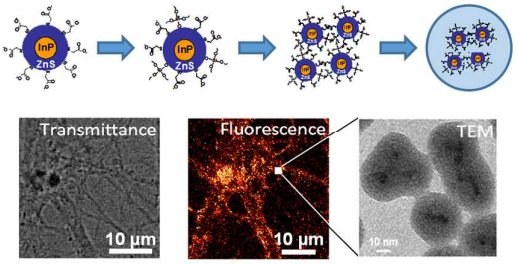

InP/ZnS quantum dots incorporated by an optimum way in silica capsules are robust and bright, and can image cells clearly